Journal of Polymers and the Environment
https://doi.org/10.1007/s10924-023-03008-4

ORIGINAL PAPER

Effect of Polymeric Nanocomposite on Sandy Soil Sta-Bilization

Zahra Feizi[1] · Abolfazl Ranjbar Fordoei[1] · Alireza Shakeri[2] · Sima Sepahvand[3]

Accepted: 23 July 2023

Abstract
Soil erosion is a threat to the inhabitant of arid and semiarid regions Soil and sand dune stabilizationusing different materials and methods is one of the main challenges of land degradation management in this area. This study assessed the possibility of using polymeric nanocomposite (acrylic acid co-acrylamide) assisted by nanofiber as mulch on the properties of sand dunes, which were polymerized by free radicals. One liter of the polymeric nanocomposite was sprayed on sample metal trays at 1wt. %, 3 wt%, and 5 wt% levels and cured for 30 days to investigate their effects on sand properties. The polymeric nanocomposite was also sprayed in one layer on some trays and two layers on other trays to compare the impact of spraying frequency. The research used a completely randomized design, with each experiment conducted three times. The effects of mulches on the treatment characteristics were examined via a wind tunnel, compressive and shear resistance, and crust thickness tests. The wind tunnel results showed the erosion rate after adding the polymeric nanocomposite was 0 g/h 0.3 m^2 at a wind velocity of 15 m/s. Furthermore, the mechanical strength of the treated samples after 30 days revealed that the 3 wt% polymeric nanocomposite improved the erodibility of treatments substantially more than the 1 wt% and 5 wt%. Accordingly, a polymeric nanocomposite of 3 wt% applied in two layers increased the compressive resistance, shear resistance, and crust thickness by 2.4, 1.94, and 16.93 times, respectively, compared to the control samples. The result improved the understanding of the effectiveness of polymeric nanocomposite in soil erosion control and is recommended to stabilize sand dunes.

Keywords Nanocomposite · Nano fiber · Chitin · Soil erosion · Sand resistance

Introduction

Arid and semiarid areas cover approximately one-third of the global landscape [1, 2]. These regions include a quarter of existing sand dunes and 17% of the world's population. Sand dunes arecharacterized by a loose fabric structure [3] and are extremely vulnerable to wind erosion. Wind erosion, accounting for approximately 60% of desertification [2, 4] could be considered a worldwide environmental driver. Every year, wind erosion destroys about 500 million hectares of the world's land, producing 500 to 5000 megatons of dust [5] and devastating the land's productive capacity through wind erosion and desertification [6]. It is a serious threat to sustainable agriculture, causing roads to be buried, canals and reservoirs to be filled, and buildings and facilities to be buried in arid and semiarid regions of the world [7]. Sand stabilization and planting and growing of plants, on the other hand, are the most critical factors in reducing damage [8]. Various physical, chemical, and biological methods are used to control wind erosion and mitigate its effects. Physical methods are primarily based on engineering technology to increase the roughness of sand surfaces and their strength through the surface covering. But this method is very costly in terms of manpower and resources. The biological method of planting and creating micro-organisms for sand stabilization has limitations due to the dry conditions of the environment and lack of water [9]. Researchers have evaluated various materials for more than half a century to find

✉ Zahra Feizi
zahra.feizi08@gmail.com

[1] Department of Desert Management and Controlling, Faculty of Natural Resources and Earth Sciences, University of Kashan, Kashan, Iran

[2] School of Chemistry, College of Science, University of Tehran, Tehran, Iran

[3] Department of Bio Systems, Faculty of New Technologies and Aerospace Engineering, Shahid Beheshti University, Zirab Campus, Tehran, Iran

Published online: 08 September 2023

Table 1 The basic physical parameters of the materials

Materials/physical parameter	Chemical formula	Molar mass (g/mol)	Melting temperature (°C)	Density (g/cm^3)
Acrylic Acid	$CH_2CHCOOH - C_3H_4O_2 - CH_2=CHCOOH$	72.06	14	1.05
Acrylamide	$CH2=CHC(O)NH_2$	71.08	84.05	1.13
Ammonium persulfate	$(NH_4)2S_2O_8$	228.21	120	1.98
Methylenebisacrylamide	$C_7H_{10}N_2O_2$	154.169	173.7–185.9	1.235

a suitable stabilizer for wind erosion control. Nowadays, chemical methods of sand stabilization or stabilizers have attracted much attention due to their ability to control wind erosion. Stabilizers are substances that are added to the soil surface to improve their mechanical properties. There are two kinds of stabilizing agents: traditional and non-traditional. Widely popular traditional additives include physical barriers [4], petroleum oil [10], fly ash, and lime [9], which are cheap, available, and effective in improving soil properties but increase soil pH and are not environmentally friendly [9, 11]. However, non-traditional additives, including composites, polymers, enzymes, etc., are increasingly being used for civil and military purposes. In addition to the chemical properties of sand stabilizers, these stabilizers create three types of crust: solid, flexible, and elastic, all three of which protect the sand surface from direct wind erosion, water evaporation, and stabilize the sand [12]. Soil stabilizers improve the engineering behavior of the soil by establishing multiple connections between the soil`s minerals and organic particles and its polar end groups, such as calcium ions [13–16]. Today, non-oil polymer, i.e., acrylate-based polymers (hydrogel), is widely used in mulches due to their minimal side effects and environmental safety. Ideal chemical stabilizers should have good adhesion and permeability, be low cost, non-polluting, and easy to produce and use [17]. Many studies have been done worldwide on how different sand dune mulches affect wind erosion [6, 11, 18, 19].

A polymer with different properties and conformations is usually formed via the polymerization of monomers [18]. Hydrogels are polymeric materials with a three-dimensional structure that contain hydrophilic functional groups [19–22]. They possess various properties, including water permeability, biodegradability, and adaptability to environmental conditions [23]. In addition, this material can absorb and store water [24, 25]. However, hydrogel's low mechanical resistance is a major limitation of its use. A nanocomposite hydrogel can solve this problem [25, 26]. Nanostructures are a good choice for polymeric networks because of their high surface area [27–29].

In this study, nano fiber of chitin was used to prepare a polymeric nanocomposite. Nano fiber has a good dispersion property in aqueous solutions and can modify some properties of hydrogels [30]. Nano chitin fiber is one of the natural biopolymers that has received attention due to its nano size, surface and mechanical properties, biodegradability, high specific surfaces, and low density [31]. Nanofiber is a reinforcing agent that interacts well with hydrophilic polymers and is a biodegradable, biocompatible, renewable, and environmentally friendly material. The high surface area of nanofiber and its strength help create a nanocomposite with better properties than the pure base material. However, the main issue with improving the nanocomposite is that by adding nano structure to the polymer, the solution's viscosity increases, and the polymer's mobility decreases [30, 32].

Table 2 Chemical properties of treated sand

Properties	EC (dS/m)	pH	SAR	Organic Matter (%)
Treated sand	2.9	7.5	2	1

This study aimed to assess the optimal concentration of polymeric nanocomposite in sand stabilization and determine its effect on sand stabilization during wind erosion. In this regard, FT-IR Spectroscopy and XRD Pattern were used to characterize the polymeric nanocomposite. Field emission scanning electron microscopy (FE-SEM) was also used to examine the composite's surface morphology in the presence of the chitin nanofiber. Anti-wind erosion tests were also applied to investigate the effect of nanocomposite concentration on the strength of the stabilized sand; the results were then used to determine the optimal nanocomposite of hydrogel dosage.

Materials and Methods

Materials

The acrylic acid, acrylamide, ammonium persulfate (APS), N, N′-methylenebisacrylamide (MBA), sodium hydroxide (NaOH), and absolute ethyl alcohol were of analytical grades and were purchased from the Merc and Sigma Aldrich companies. The nanofiber chitin (NFCH) was purchased from the Nanonovin Polymer Company (Mazandaran, Iran). Table 1 shows the basic physical parameters of the materials.

Tested sand

The sand dunes samples used in this study were formed during the Quaternary period and collected from the Siyazgeh Desert (Abuzeidabad) in Isfahan province (Fig. 1), Iran, at a depth of 0–10 cm. The chemical properties, including EC, pH, SAR, and organic matter, were identified based on the American Standard Test Mesh (ASTM) (Table 2). The samples were classified as fine sandy according to the American Standard Test Mesh (ASTM). The grain size analysis performed to determine the soil's sand properties indicated the existence of 80% sand particles.

Polymeric Nanocomposite

A set of polymeric composites based on nanofiber, acrylic acid, and acrylamide was synthesized using free radical graft copolymerization in the presence of MBA and APS as a crosslinker and an initiator, respectively. The synthesized method was done according to the following procedure [33]: firstly, 10 g nanofiber of 10 wt% was dispersed into 15 ml distilled water by ultrasonic vibration for 1 h. Then, acrylic acid (1 g) was dissolved in deionized water (15 mL) at 80 °C in a three-necked flask with a magnetic stirrer and a nitrogen line. Simultaneously, NaOH (0.5 g) was dissolved into the mixture solution. Thereafter, acrylamide (0.25 g), MBA (0.009 g), and ASP (0.06 g) were subsequently added to the reaction mixture. The whole solution was stirred for 30 min (T2). Amounts of 30 and 50 g nanofiber were used for production treatments 3 and 4, respectively.

Test Methods

Sand Stabilization Using Polymeric Nanocomposites

Different concentrations of the polymeric nanocomposites (1, 3, and 5 wt%) were used to investigate the efficiency of the polymeric nanocomposites on the samples with three replications. Accordingly, the sand samples were first flatted in 100×30×2 cm metal trays. These samples were tested under dry moisture conditions. Three different concentrations (1, 3, and 5 wt%) of the polymeric nanocomposites were mixed with 1 L of tap water, and then these solutions were sprayed onto the surface of the trays (l/0.3 m^2). A spray pistol attached to a 2.5-liter tank uniformly sprayed the mulches on the sand surface. In two-layer treatments, the first layer was sprayed and let dry, and the second was applied. Finally, the trays were kept and dried at room temperature in the laboratory before exposure to the wind erosion test to specify the friction velocity threshold. Polymeric composites without nanofiber (T1) and water (T0) were sprayed onto the samples in the control samples. All treatments are summarized in Table 3.

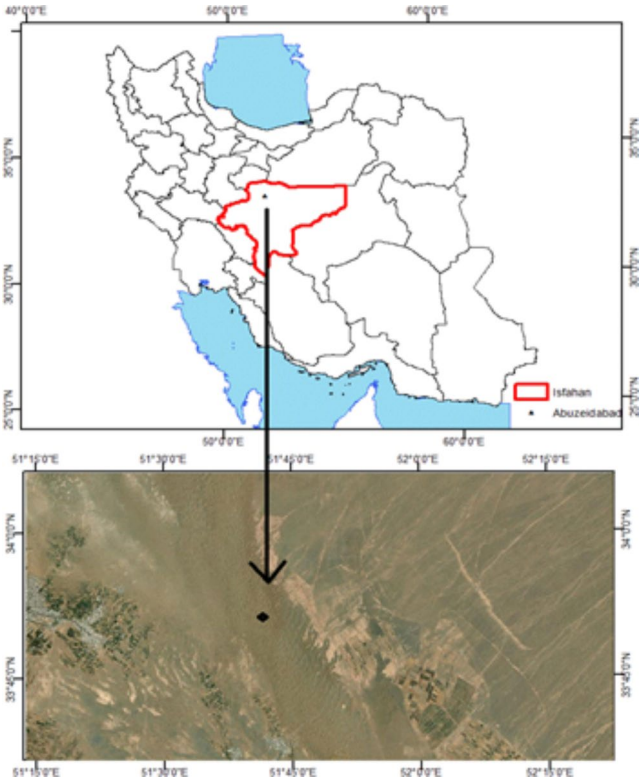

Fig. 1 The image of the sampling area on the map of Iran and Isfahan province

Wind Tunnel test

A wind tunnel was employed to capture the erodibility of samples to wind erosion at the Tehran University wind

Table 3 Preparation conditions of the samples

One layer				Two layers			
Treatment	AA+AM[1] (%)	NFCH[2] (%)	code	Treatment	AA+AM (%)	NFCH (%)	Code
Control 1	1	0	T1	Control 2	0	0	T0
polymeric nanocomposites	1	1	T2	polymeric nanocomposites	1	1	T5
	1	3	T3		1	3	T6
	1	5	T4		1	5	T7

[1] Acrylic Acid co Acrylamide.

[2] Nanofiber Chitin.

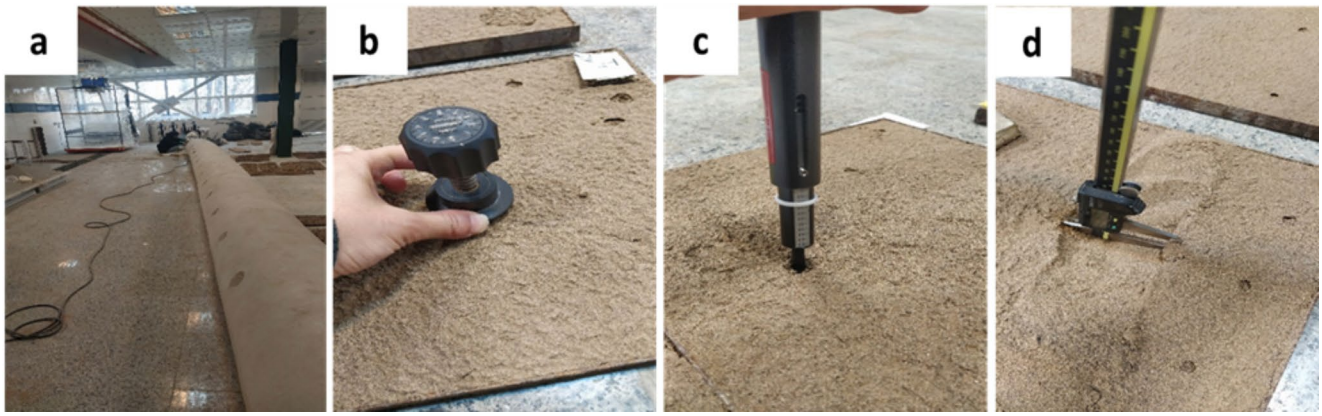

Fig. 2 Measurement device: (**a**) wind tunnel, (**b**) shear tester, (**c**) hand cone penetrometer, and (**d**) caliper

tunnel laboratory. This device consists of three sections: wind generator (blower), test section, and sediment chamber (Fig. 2a) [9]. The wind-generating fans are located in the first section, and the maximum wind speed created by this device is 15 m/s. The sample trays were placed in the device's second part, located at a distance from the fan. The third section consists of a 10-meter-long plastic chamber for the deposition of sand carried by the wind.

Shear Resistance test

Soil erosion control methods generally consist of increasing the strength of the soil surface to maximum external stress while maintaining structural integrity [16]. This study measured the shear strength by pushing a Geo Torvane shear tester into the soil surface at about an 8 mm depth at three points in each sample. A Geo Torvane shear tester is a device with the ability to measure stress between 0 and 250 kPa (Fig. 2b) [34]. The shear resistance is determined by applying pressure and rotational force to break the crust. The amount of stress value is determined by the dial at the top of the device [34].

Penetration Resistance test

The soil mechanical resistance is the amount of soil compression measured by soil penetration resistance [35, 36]. This study used a hand cone penetrometer to estimate soil penetration resistance (Fig. 2c). The penetrometer determined the force needed to advance a specific base-size cone into the soil [36]. Penetration resistance was measured at 10 random points in each tray.

Crust Thickness test

Using mulch causes the sand particles to bond together and create a crust. The thickness of the crust was determined at five points of each tray using a caliper (Fig. 2d). It should be mentioned that the loose sand attached to the sub-layer was separated from it by abrasion before the actual thickness was determined [36].

Table 4 Statistical results for the measured properties across the different treatments

Index	Sum of Squares	df	Mean Square	F	Sig.
shear strength	8.52	7	1.22	374.62	< 0.0001*
compressive strength	16.96	7	2.42	5.30	0.0028*
crust diameter	604.38	7	86.34	318.24	< 0.0001*

* Indicates a significant difference at the 5% level

Data Analysis

This study was conducted using a randomized complete block design with three replications. Analysis was done using SPSS (Ver. 20.0) and multiple mean comparisons using Duncan's multiple range test. Excel software (version 2013) was used to draw the graphs. According to Table 4, the P-value was estimated for each test [36].

Results and Discussion

FTIR Characterization

As presented in Fig. 3, the Polymeric nanocomposite and also control sample (AA-AM) were explored using FTIR to confirm the identification of functional groups. As shown, in AA-AM spectra, the strong peaks at ~ 3351 cm^{-1} and 1556 $cm^{-1,}$ are related to the stretching vibration of hydroxyl groups (O-H) and asymmetric stretching vibration of carboxyl groups (COO^{-}), respectively [38]. The peaks observed at 1488 cm^{-1} correspond to the $–CH_2$ groups. The sharp peak at 1731 cm^{-1} attributed to the stretching vibration of carbonyl groups (C = O) of carboxylic acid in acrylic

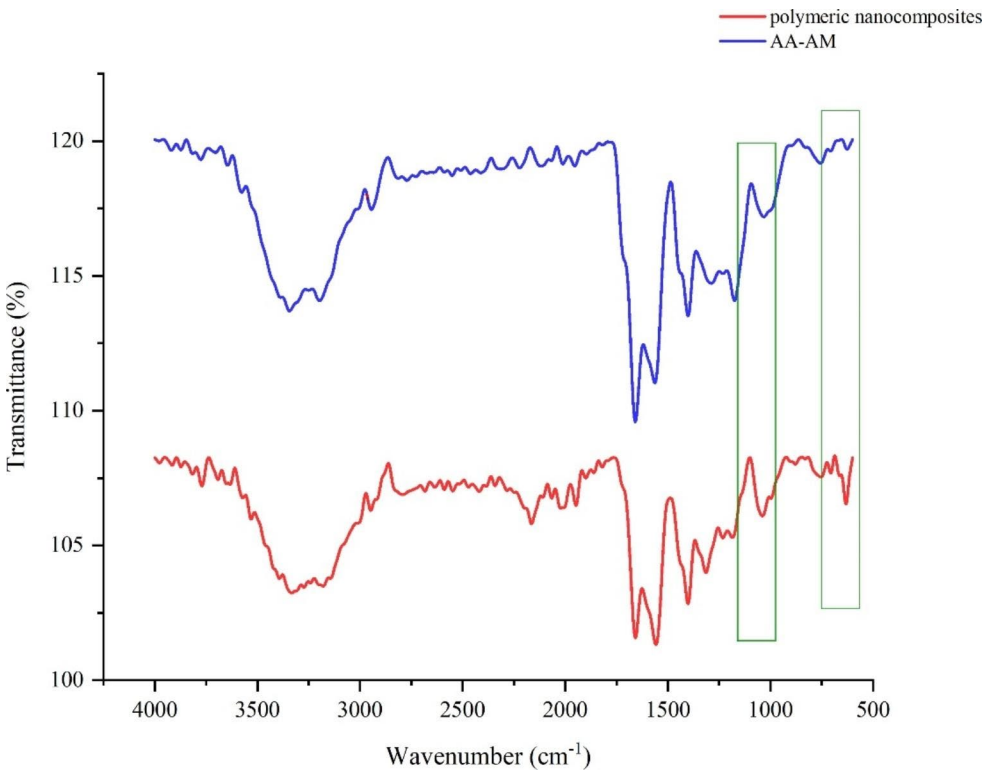

Fig. 3 FTIR of Polymeric nanocomposite and AA-AM

acid [37], while a small peak at ~2946 cm^{-1}, corresponds to the asymmetric stretching vibration of C–H [14, 39, 42, 43]. Compared with AA-AM, some new peaks observed in polymeric nanocomposites at 1044 cm^{-1} and 635 cm^{-1} corresponds to the C–O band in the $–OCH_3$ groups [39]. Small peak at ~2946 cm^{-1} in AA-AM spectra vanished in polymeric nanocomposites, while the peak at 1488 cm^{-1} shifted to higher wavenumber at 1563 cm^{-1}. This behavior might be related to the graft-copolymerization of synthesized monomers with cellulose fibers. Thus, the new peaks in the polymeric nanocomposites spectrum illustrates that chemical modification occurred, revealing the functional groups of the nanofiber chitin that successfully transferred onto AA-AM. The shifted bands observed at 1565 cm^{-1} and 1563 cm^{-1} were attributed to the successful graft polymerization of acrylamide monomer [44] and C = O asymmetric stretching in the carboxylate anion [45]. Overall, the FTIR results analysis that the polymerization and the response of composite formation were successfully captured. The presence of these functional groups on the polymer chain causes their polar interactions with sand particles. According to the results, the number of binding functional groups was increased by increasing the amount of hydrogel to a certain amount indicating that the crusts were formed stronger [46].

FE-SEM

Figure 4 shows an FE-SEM micrograph of the polymeric nanocomposite. The results showed that the polymeric nanocomposite has a porous and three-dimensional structure. The pores are where water percolation and the interaction of external stimuli and hydrophilic soil groups occur [38]. The FE-SEM image comparison clearly shows that the small pores contribute to specific surface area increases [39]. Figure 4 illustrates the structural difference of the polymeric nanocomposite, including the porosity. Generally, a dense structure increases and decreases specific surface area and pore size, respectively, indicating which shape carries the highest specific surface area. Also, it is observed that the polymeric nanocomposite surface benefits from a reasonably porous matrix associated with relatively good dispersion and higher specific surface areas than the AA-AM [40]. Our FE-SEM findings indicated that the surface morphology of the acrylate hydrogel (AA-AM) changed in the presence of the nanofiber, confirming proper interaction and conformity between NFCH and AA-AM.

X-ray Diffraction (XRD) Pattern

The XRD Patterns of the composite are displayed in Fig. 5. The X-ray diffraction (XRD) Pattern of the composite presents diffraction peaks corresponding to the crystalline phase of fiber, indicating the proper distribution of nanofiber in

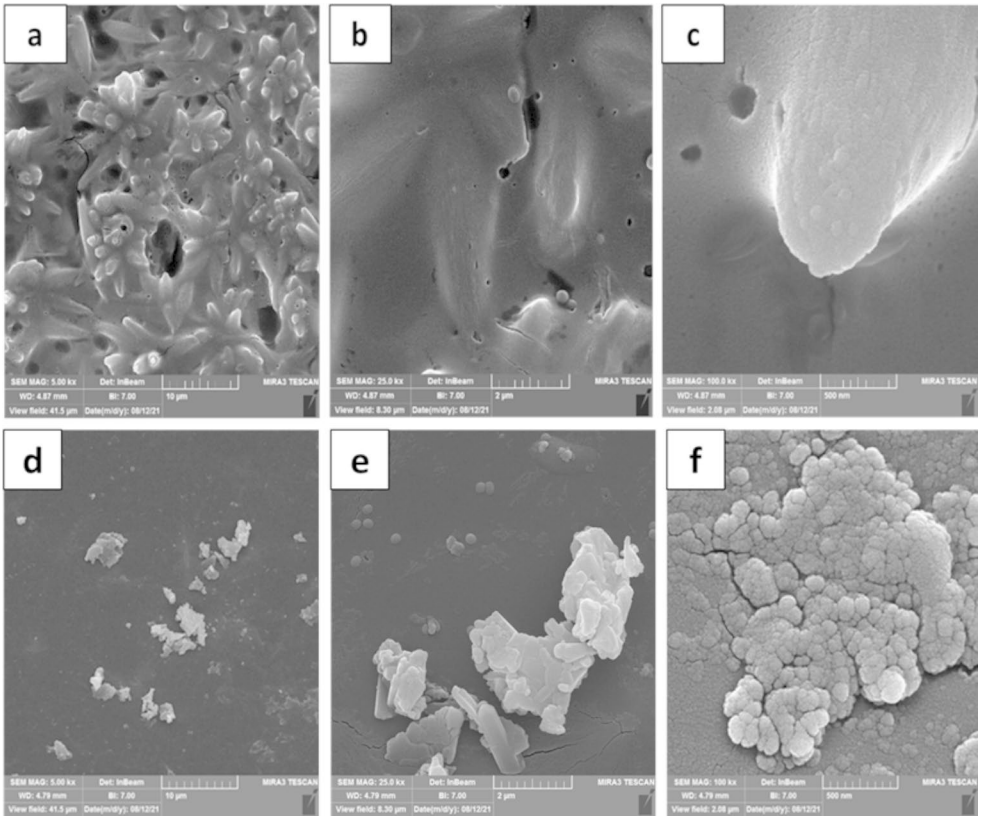

Fig. 4 FE-SEM of Polymeric nanocomposite with different magnifications, (**a**) 5 kx, (**b**) 25 kx, (**c**) 100 kx, and FE-SEM of AA-AM with different magnifications (**d**) 5 kx, (**e**) 25 kx, and (**f**) 100 kx

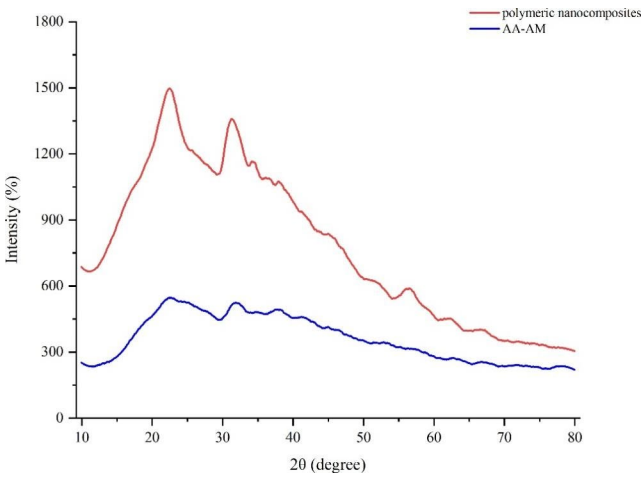

Fig. 5 X-ray diffraction (XRD) patterns of Polymeric nanocomposite and AA-AM

the polymer chains. As presented in Fig. 5, the composite had a main characteristic peak angle of 22.5˚, 31.5˚, and 56˚, respectively. The sharper and more intense peaks in the polymeric nanocomposite mean more crystallinity in that sample [41]. As can be seen in Fig. 5, the different XRD patterns for AA-AM and polymeric nanocomposite were captured, indicating that the chitin nanofiber significantly affected the polymeric nanocomposite crystalline structure. This pattern for previous samples of windy sand indicated that the sand only contains quartz [42], while the XRD analysis of the crusts containing the polymeric nanocomposite indicates the presence of a calcium carbonate group ($2\theta = 30^{\circ}$) as a sand particles connector [42].

Threshold Friction Velocity Test

After preparing the treatments and transferring the tray to the wind tunnel, the erodibility of the treatments was investigated. The erodibility of both control and treatment samples was examined under the different wind velocities. In short, the wind speed was gradually increased until the wind power detached the sand particles from the sample surfaces. The relative wind erodibility of each treatment was specified concerning the threshold friction velocity. The threshold friction velocity for the control sample (T0) was evaluated at 5 m/s. The erosion rate for the irrigated control sample (T0) was gradually increased with exposure to stronger wind due to increased wind erosion power and the high erodibility of sand particles. The erosion rate of the irrigated sample (T0) by increasing wind velocity was between 3.5 g/h 0.3 m^2 and 9 g/h 0.3 m^2; the samples treated with mulch were 0 g/h 0.3m^2 at maximum wind velocity

(15 m/s). The mulches have a hydrogel structure, as shown by Kargarzadeh et al.[38, 43] and Mahdizadeh et al. [38, 43], attributed to their ability to retain moisture and create a connection between soil particles preventing them from being removed by the wind. Moreover, the polymeric nanocomposite covered the sand particles, increasing the anti-wind properties of the sand. Li et al. also suggested that sand aggregation and crusts produced by a polymer composite increased anti-wind erosion ability [4]. The polymeric nanocomposite`s hydrophilic groups give it the ability to absorb and retain water preventing the soil surface from drying out. This allows hydrogen bonding between sand particles, making them stronger against wind erosion, at least until they lose the water [24]. The results of increasing the threshold friction velocity using polymer have been proven by many researchers, including Bakhshi et al. [44], Zomorodian et al. [45], and Yang et al. [7].

Shear Strength

The Duncan test results showed a significant difference in the mulches' shear strength ($P < 0.05$). As shown in Fig. 5, the shear properties of the stabilized sandy soil samples improved relative to the control sample. Based on Duncan's test results, the mean comparisons showed that T6 (1.94 N/cm^2) received the highest shear, while there were no substantial differences between the T2 and T4 treatments. The shear strength increased by 0.71 and 0.77 N/cm^2 for these two treatments, respectively, compared to the control samples (T1 and T0). The T0 treatments received the lowest shear strength but differed only slightly from that observed for T1, indicating the effectiveness of nanofiber as a polymeric nanocomposite reinforcement in enhancing the shear strength of the samples. Also, it can be seen that the shear resistance improved significantly in the samples with a second sprayed layer. The presence of the polymeric nanocomposite between soil particles makes multiple contacts with the soil's mineral and organic particles, fixing the soil structure and enhancing the soil's resistance ability. This is consistent with the results reported by [14, 17, 46–48], who also reported that multiple contact between particles affects shear strength. Moreover, polymeric nanocomposite contains sodium carboxylate, which increases the cation exchange capacity (CEC) of the samples, which in turn, influences the strength of the stabilized soil due to the ionization occurring on the sand surface. The same outcome was reported by Jing et al., who showed that a hydrogel composite sustains soil crusts [24]. Horn et al. showed the particle connection and their surface properties' effect on the soil resistance to external stress [49].

Considering the consequences of this study, as discussed above, it can be argued that polymeric nanocomposite concentration played a dominant role in the bonding of sand particles. Using the geo Torvane shear tester (shear strength test) found that setting the proper dosage of nanocomposite solutions can intensify the strength and stiffness of sands [3, 17, 50, 51]. An excessive dosage of nanostructure may result in composite aggregation and reduce the mechanical properties [52, 53]. This phenomenon is explained by the fact that an excessive dosage of nanofibers can become clumped due to van der Waals forces leading to aggregation and reducing the composite`s quality by creating poor surface adhesion between the nanocomposite and sand particles. Several studies reported that increasing the nanofiber first improved the shear resistance, but when more nanofiber was added, the shear resistance decreased [54–56]. In this study, the polymeric nanocomposite of 3 wt% had the highest shear resistance. As shown in Fig. 6, the mulches with two layers of polymeric nanocomposite in the same concentration were determined to be a more resistant treatment. This can be explained by hydroxyl groups within the polymer's chain, making hydrogen bonds on the surface and within the space between sand particles. Otherwise, the water absorption capacity will increase as the hydrogel increases due to the polymeric nanocomposite's amount of spraying. Increases in hydroxyl groups and, therefore, the hydrogen bonds among the sand particles improve the intermolecular resistance, creating a thicker and harder crust and improving the samples' erodibility [42, 57]. This finding is consistent with the results reported by Meng et al. and Zare et al., who also reported hydrogen bonds on the sand surface and intermolecular forces that attached sand particles and created a harder crust [9, 58]. Mombeni et al. (2021) reported that two layers of bagasse lignocellulosic microfibers had the highest shear and penetration resistance [36]. Khalili Moghadam et al. (2015) demonstrated the mulch`s penetration increases by increasing the thickness of the mulch [34]. Diouf et al. also reported wind erosion resistance increases with the thickness of mulch layers [59].

Crust Diameter

Duncan`s test showed a difference between mulches for one and two layers sprayed, but this difference is insignificant. Comparing control samples T1 and T0 showed crust thickness increased at least 13 times for the sample treated with polymeric composite without nanofiber (T1) compared to T0. More crust thickness was observed in the double layer sprayed 3 wt% polymeric nanocomposites (16.93 ± 1.88 mm). As observed in Fig. 6, the thickness of the formed crust increased as the concentration of polymeric nanocomposite was increased to 3 wt%; however, increasing the concentration after that did not lead to an increase in crust thickness. The greatest crust thickness was observed in

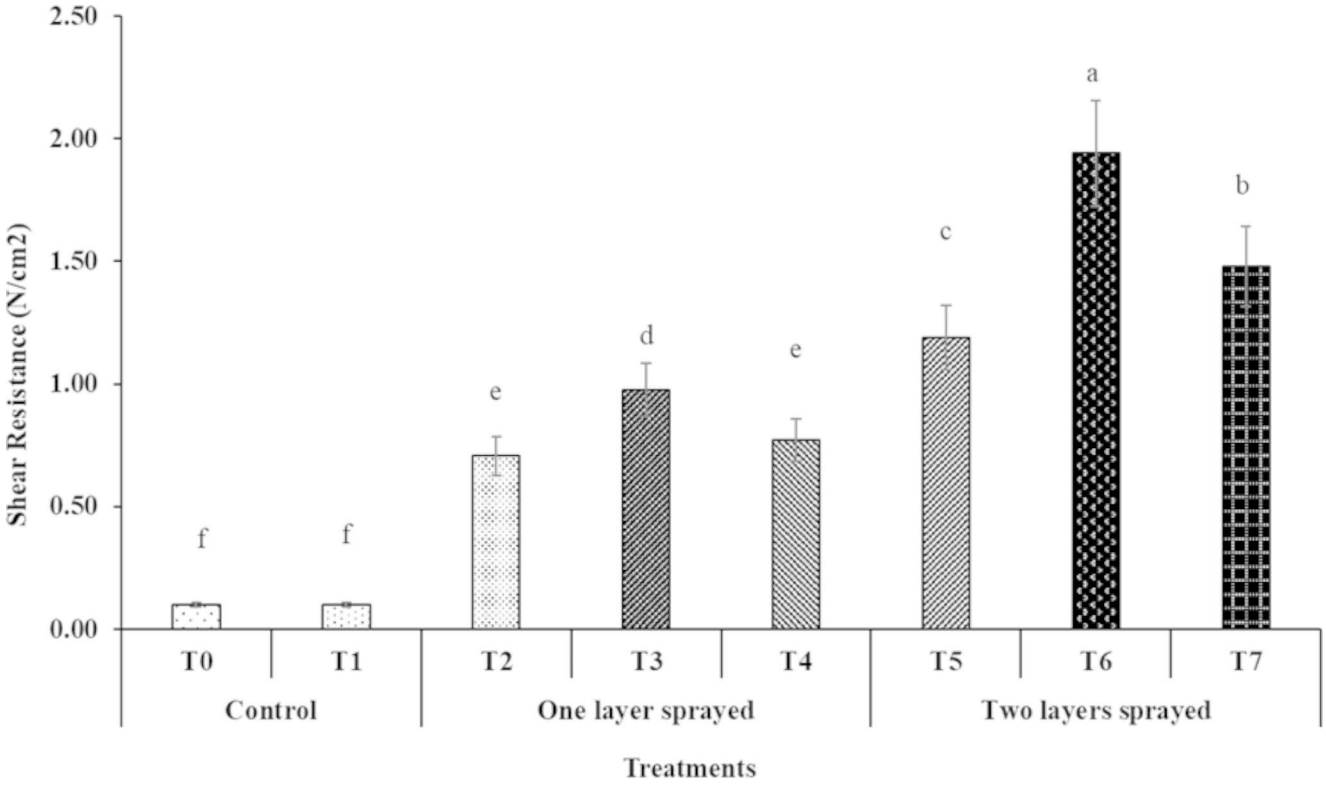

Fig. 6 Effect of different concentrations and amounts of polymeric nanocomposite on shear resistance (Averages with at least one letter in common do not have a significant difference)

the sample treated with a 3 wt% polymeric nanocomposite, which is consistent with the results of Almajed et al. Their research showed that increasing the amount of composite polymer does not increase the thickness of the crust. This indicates that increasing the nanofiber increases the viscosity, diminishing the osmotic effect [60], so penetration depth decreases and creates a thinker crust. The same result was observed by Robichaud et al. and Nascimento et al., who showed that an increase in viscosity due to increasing concentration could reduce the mobility of the polymer chain [30, 32]. Therefore, the T3 and T6 samples created a thicker crust than other treatments. This result is well established in Fig. 7.

Penetration Resistance

Substantial differences were shown between mulches concerning their penetration resistance ($P < 0.05$) (Fig. 8). The compressive resistance significantly increased by increasing the nanostructure to 3 gr/0.3 m^2 ($P < 0.05$). More penetration resistance was observed in T6 (2.4 ± 0.27 kg/cm^2), and less resistance was shown in T0 (0.3 ± 0.03 kg/cm^2). The sand combines the macroporous (> 10 microns), micro, and mesoporous (60 nm–10 µm), and the polymeric nanocomposite fills up the smallest space between the sand particles, bonding them, creating a membrane and improving their strength. The increase in compressive strength from increasing the amount of nanofiber up to 3 wt% can be justified by the fact that adding nanofiber to the polymeric nanocomposite causes load transfer from the surface of the polymer to the reinforced part of the nanofiber. Since the nanofiber is much stronger than the polymer part of the nanocomposite, it strengthens the polymer, increasing its compressive strength. Additionally, the specific surface area of nanofiber is high, so the polymer, as a connector between sand particles, can create more connections.

Conclusions

Through this study, the polymeric nanocomposite was synthesized by polymerization of acrylic acid and acrylamide onto nanofiber. In the first step, polymer analyses showed that the polymeric nanocomposite is a porous structure with more surface area than AA-AM; the FE-SEM supports this idea. According to the FTIR results, the composite formation reaction and polymerization were successfully accomplished. FTIR and XRD patterns indicated the existence of different functional groups (hydroxyl, carboxyl, carbonyl, sodium, calcium carbonate, etc.) in the composite structure, causing the polymer to interact with sand particles. In the second step, the effect of different concentrations of

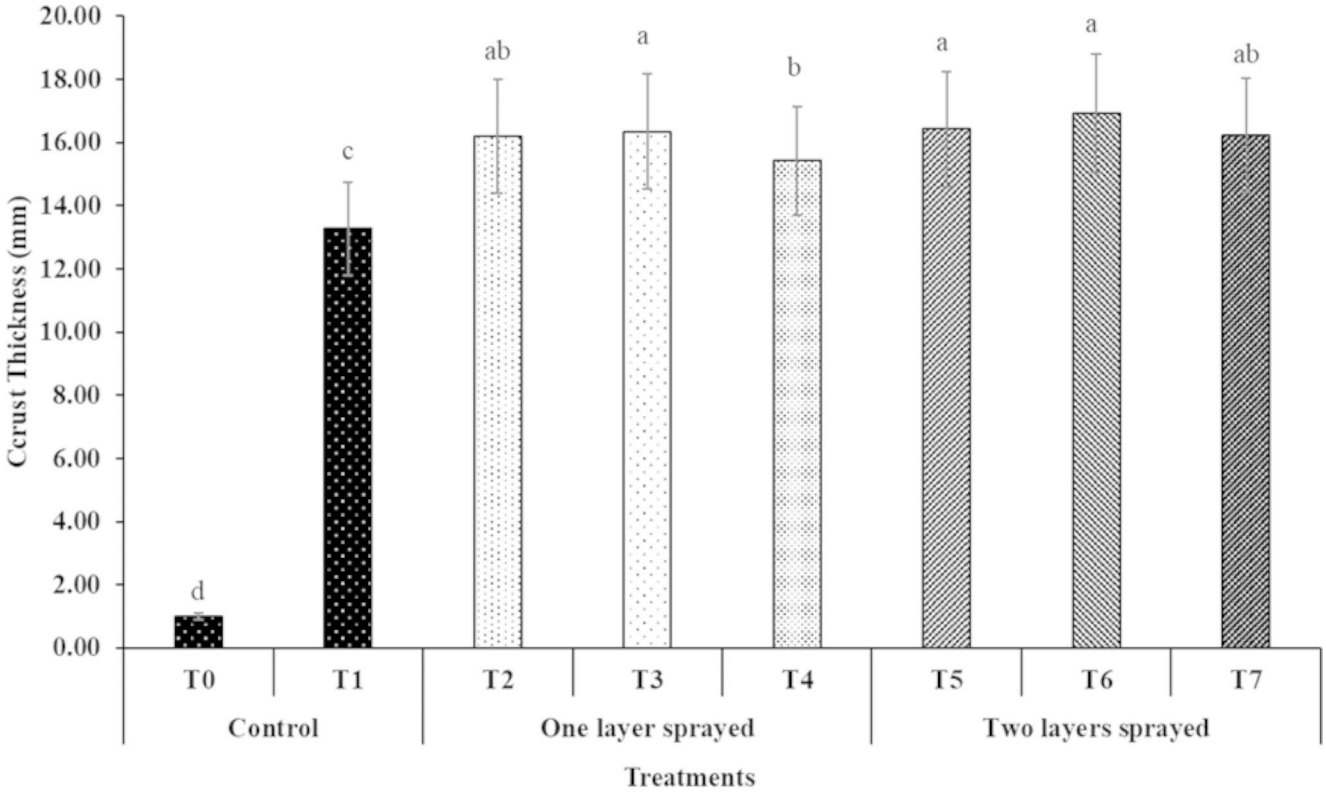

Fig. 7 Effect of different concentrations and amounts of polymeric nanocomposite on crust thickness (Averages with at least one letter in common do not have a significant difference)

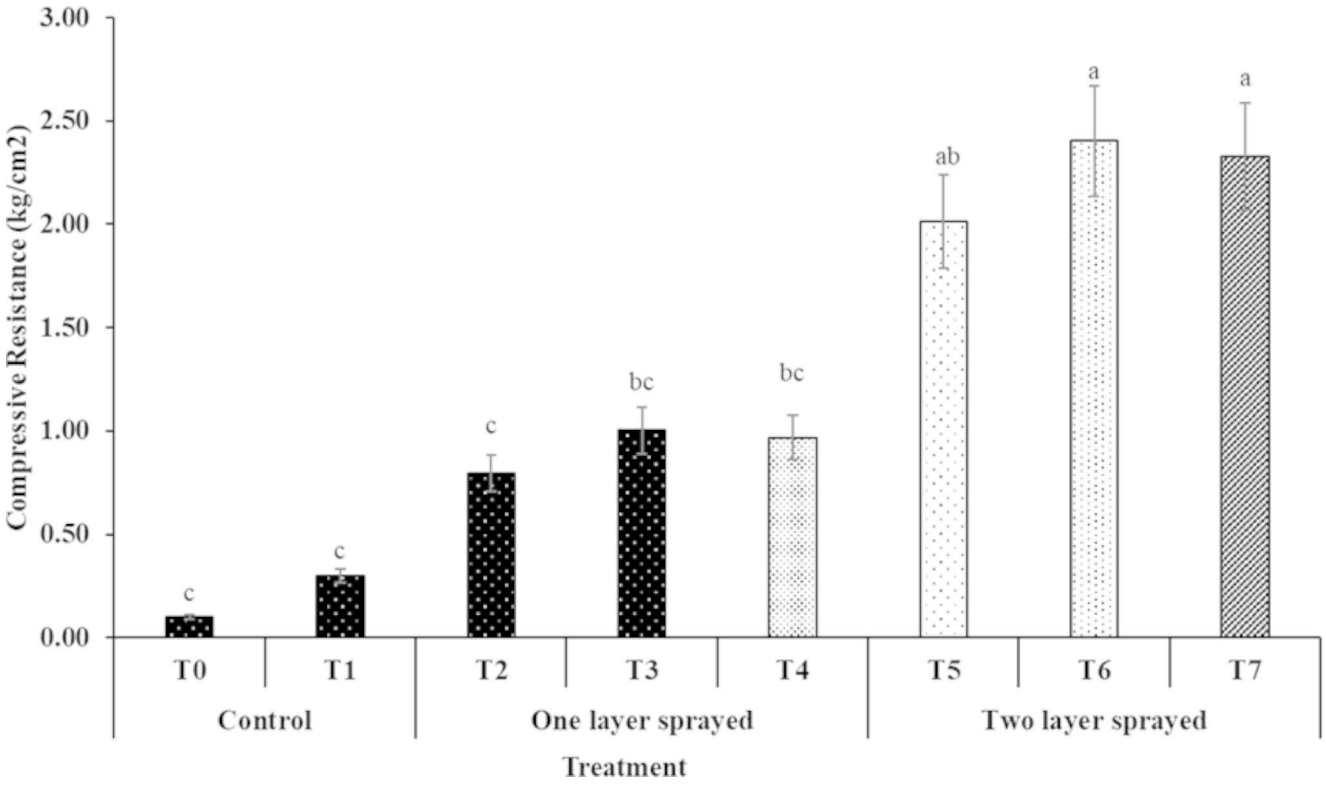

Fig. 8 Effect of different concentrations and amounts of polymeric nanocomposite on compressive resistance (Averages with at least one letter in common do not have a significant difference)

polymeric nanocomposite on anti-wind erosion was studied. Data analysis revealed that all treatments significantly affected soil erodibility, and soil erodibility decreased with the application of the polymeric nanocomposite more than AA-AM. The wind tunnel test showed that the specimens' threshold friction velocity increased with polymeric nanocomposite utilization; this phenomenon is explained by the fact that the nanocomposite covers all of the sample's area, increasing the sand particles' connection due to functional groups observed in the polymeric nanocomposite. This indicates the existence of different functional groups (hydroxyl, carboxyl, carbonyl, sodium, calcium carbonate, etc.) in the composite structure, causing the polymer to interact with sand particles. The addition of the polymeric nanocomposite to the sand samples improved its mechanical capacities, which were determined by sand resistance tests. From the strength aspect of sandy soils, the optimum composite content was estimated at 3 wt% nanofibers since it yielded the best results in all tests. The strength of sand samples decreased as the increment of nanofiber contents increased up to about 5 wt%, where the strength of the sand samples became weaker. This phenomenon is explained by the fact that the nanofiber of the composite accumulated due to the van der Waals forces leading to the formation of poor clusters and increasing viscosity, and finally, poor surface adhesion between sand particles. In this study, treatments of a double-layer spray of the polymeric nanocomposite were determined as more resistant than one layer. The study's conclusions were derived from laboratory experiments only; therefore, field studies and tests will be required to verify them.

Acknowledgements The authors are very grateful for the support of Tehran University for this research. The laboratory study of this research was carried out in the laboratory of the Department of Revitalization of Dry and Mountainous Areas and the Department of Chemistry.

Author Contributions Zahra Feizi: ideatin, conceptualization, methodology, data curation, writing. Alireza Shakeri and Abolfazl ranjbar: the theory's develoption, supervision. Sima Sepahvend: writing, validation.

Declarations

Competing Interests The authors declare no competing interests.

References

1. Chen W, Dong Z, Li Z, Yang Z (1996) Wind tunnel test of the influence of moisture on the erodibility of loessial sandy loam soils by wind. J Arid Environ 34. https://doi.org/10.1006/jare.1996.0119
2. Liu J, Shi B, Lu Y et al (2012) Effectiveness of a new organic polymer sand-fixing agent on sand fixation. Environ Earth Sci 65. https://doi.org/10.1007/s12665-011-1106-9
3. Mohamedzein Y, Al-Hashmi A, Al-Abri A, Al-Shereiqi A (2019) Polymers for stabilisation of Wahiba dune sands, Oman. Proc Inst Civil Eng Ground Improv 172. https://doi.org/10.1680/jgrim.17.00063
4. Li Y, Cui J, Zhang T et al (2009) Effectiveness of sand-fixing measures on desert land restoration in Kerqin Sandy Land, northern China. Ecol Eng 35. https://doi.org/10.1016/j.ecoleng.2008.09.013
5. Thomas GW (1996) Methods of Soil Analysis. Part 3. Chemical Methods. Methods of Soil Analysis. Part 3. Chemical Methods, SSSA and ASA, Madison, WI
6. Chang I, Prasidhi AK, Im J et al (2015) Soil treatment using microbial biopolymers for anti-desertification purposes. Geoderma 253–254. https://doi.org/10.1016/j.geoderma.2015.04.006
7. Yang K, Tang Z (2012) Effectiveness of fly ash and polyacrylamide as a sand-fixing agent for wind erosion control. Water Air Soil Pollut 223. https://doi.org/10.1007/s11270-012-1173-x
8. Rende W, Zhongling G, Chunping C et al (2015) Quantitative estimation of farmland soil loss by wind-erosion using improved particle-size distribution comparison method (IPSDC). Aeolian Res 19. https://doi.org/10.1016/j.aeolia.2015.06.005
9. Meng X, Liang L, Liu B (2017) Synthesis and sand-fixing Properties of Cationic Poly(vinyl acetate-butyl acrylate-2-hydroxyethyl acrylate-DMC) copolymer emulsions. J Polym Environ 25. https://doi.org/10.1007/s10924-016-0826-z
10. Hashemimanesh M, Matinfar H (2012) Evaluation of desert management and rehabilitation by petroleum mulch base on temporal spectral analysis and field study (case study: Ahvaz, Iran). Ecol Eng 46. https://doi.org/10.1016/j.ecoleng.2012.04.038
11. Song Z, Liu J, Yu Y et al (2021) Characterization of artificially reconstructed clayey soil treated by polyol prepolymer for rock-slope topsoil erosion control. Eng Geol 287. https://doi.org/10.1016/j.enggeo.2021.106114
12. Han Z, Wang T, Dong Z et al (2007) Chemical stabilization of mobile dunefields along a highway in the Taklimakan Desert of China. J Arid Environ 68. https://doi.org/10.1016/j.jaridenv.2006.05.007
13. Mirzababaei M, Arulrajah A, Ouston M (2017) Polymers for stabilization of Soft Clay Soils. In: Procedia Engineering.
14. Wei X, Ma X, Peng X et al (2018) Comparative investigation between co-pyrolysis characteristics of protein and carbohydrate by TG-FTIR and Py-GC/MS. J Anal Appl Pyrolysis 135. https://doi.org/10.1016/j.jaap.2018.08.031
15. Rezaeimalek S, Huang J, Bin-Shafique S (2017) Evaluation of curing method and mix design of a moisture activated polymer for sand stabilization. Constr Build Mater 146. https://doi.org/10.1016/j.conbuildmat.2017.04.093
16. Chang I, Lee M, Tran ATP et al (2020) Review on biopolymer-based soil treatment (BPST) technology in geotechnical engineering practices. Transp Geotechnics 24
17. Dong Z, Wang L, Zhao S (2008) A potential compound for sand fixation synthesized from the effluent of pulp and paper mills. J Arid Environ 72. https://doi.org/10.1016/j.jaridenv.2008.02.008
18. Hui B, Zhang Y, Ye L (2014) Preparation of PVA hydrogel beads and adsorption mechanism for advanced phosphate removal. Chem Eng J. 235. https://doi.org/10.1016/j.cej.2013.09.045
19. Alvarez-Lorenzo C, Concheiro A (2002) Reversible adsorption by a pH- and temperature-sensitive acrylic hydrogel. J Controlled Release. 80. https://doi.org/10.1016/S0168-3659(02)00032-9
20. Gu B, Doner HE (1992) The interaction of polysaccharides with silver hill illite. Clays Clay Miner 40. https://doi.org/10.1346/CCMN.1992.0400203

21. Mantovan J, Pereira JF, Marim BM et al (2022) Nanocellulose hydrogels. In: Industrial Applications of Nanocellulose and its Nanocomposites
22. Mohamed SWA (2004) Stabilization of Desert Sand Using Water-Borne Polymers
23. Panova IG, Ilyasov LO, Khaidapova DD et al (2020) Polyelectrolytic gels for stabilizing sand soil against wind Erosion. Polym Sci - Ser B 62. https://doi.org/10.1134/S1560090420050103
24. Jing Z, Xu A, Liang YQ et al (2019) Biodegradable poly(acrylic acid-co-acrylamide)/ poly(vinyl alcohol) double network hydrogels with tunable mechanics and high self-healing performance. Polym (Basel) 11. https://doi.org/10.3390/polym11060952
25. Nassaj-Bokharaei S, Motesharezedeh B, Etesami H, Motamedi E (2021) Effect of hydrogel composite reinforced with natural char nanoparticles on improvement of soil biological properties and the growth of water deficit-stressed tomato plant. Ecotoxicol Environ Saf. 223. https://doi.org/10.1016/j.ecoenv.2021.112576
26. Guilherme MR, Aouada FA, Fajardo AR et al (2015) Superabsorbent hydrogels based on polysaccharides for application in agriculture as soil conditioner and nutrient carrier: a review. Eur Polym J 72
27. Rivas-Orta V, Antonio-Cruz R, Mendoza-Martínez AM Hydrogels from Poly (Acrylic Acid)/Carboxymethyl CellulosePoly (Acrylic Acid)/Methyl Cellulose, Rivas-Orta V, Antonio-Cruz R, Mendoza-Martínez AM et al (2008) A.B. Morales Cepeda and M.J. Cruz-Gómez. Journal of Materials Online 4
28. Rop K, Mbui D, Karuku GN et al (2020) Characterization of water hyacinth cellulose-g-poly(ammonium acrylate-co-acrylic acid)/nano-hydroxyapatite polymer hydrogel composite for potential agricultural application. Results Chem 2. https://doi.org/10.1016/j.rechem.2019.100020
29. Spagnol C, Rodrigues FHA, Pereira AGB et al (2012) Superabsorbent hydrogel composite made of cellulose nanofibrils and chitosan-graft-poly(acrylic acid). Carbohydr Polym 87. https://doi.org/10.1016/j.carbpol.2011.10.017
30. Nascimento DM, Nunes YL, Figueirêdo MCB et al (2018) Nanocellulose nanocomposite hydrogels: Technological and environmental issues. Green Chem 20
31. Li MC, Wu Q, Song K et al (2016) Chitin nanofibers as reinforcing and Antimicrobial Agents in Carboxymethyl Cellulose Films: influence of partial Deacetylation. ACS Sustain Chem Eng 4. https://doi.org/10.1021/acssuschemeng.6b00981
32. Robichaud PR, Jennewein J, Sharratt BS et al (2017) Evaluating the effectiveness of agricultural mulches for reducing post-wildfire wind erosion. Aeolian Res 27. https://doi.org/10.1016/j.aeolia.2017.05.001
33. Ren J, Kong W, Sun R (2014) Preparation of Sugarcane Bagasse/Poly(Acrylic Acid-co-Acrylamide) Hydrogels and their application. Bioresources 9. https://doi.org/10.15376/biores.9.2.3290-3303
34. khalili moghadam B, Jamili T, Nadian H, Shahbazi E (2015) The influence of sugarcane mulch on sand dune stabilization in Khuzestan, the southwest of Iran. Iran Agric Res 34:71–80
35. Herrick JE, Jones TL (2002) A dynamic cone penetrometer for measuring soil penetration resistance. Soil Sci Soc Am J 66. https://doi.org/10.2136/sssaj2002.1320
36. Mombeni M, Reza Asgari H, Mohammadian Behbahani A et al (2021) Effect of bagasse lignocellulose microfibers on sand stabilization: a laboratory study. Aeolian Res 49. https://doi.org/10.1016/j.aeolia.2020.100654
37. Ismaeilimoghadam S, Jonoobi M, Hamzeh Y, Danti S (2022) Effect of Nanocellulose types on Microporous Acrylic Acid/Sodium Alginate Super Absorbent Polymers. J Funct Biomater 13:273. https://doi.org/10.3390/jfb13040273
38. Kargarzadeh H, Ioelovich M, Ahmad I et al (2017) Methods for extraction of Nanocellulose from various sources. In: Handbook of Nanocellulose and Cellulose Nanocomposites
39. Chen Y, Li Q, Li Y et al (2020) Fabrication of cellulose nanocrystal-g-poly(acrylic acid-co-acrylamide) aerogels for efficient pb(II) removal. Polym (Basel) 12. https://doi.org/10.3390/polym12020333
40. Sepahvand S, Bahmani M, Ashori A et al (2021) Preparation and characterization of air nanofilters based on cellulose nanofibers. Int J Biol Macromol 182. https://doi.org/10.1016/j.ijbiomac.2021.05.088
41. Sepahvand S, Jonoobi M, Ashori A et al (2020) Surface modification of cellulose nanofiber aerogels using phthalimide. Polym Compos 41. https://doi.org/10.1002/pc.25362
42. Almajed A, Lemboye K, Arab MG, Alnuaim A (2020) Mitigating wind erosion of sand using biopolymer-assisted EICP technique. Soils Found 60. https://doi.org/10.1016/j.sandf.2020.02.011
43. Mahdizadeh M, Najafi N (2018) Applications of Nanomaterials in Soil Remediation. Land manegment 6:31–48
44. Bakhshi MM, Ayati B, Ganjidoust H (2021) Soil stabilization by Nano Polymer Polylatice (Case Study: Hossein Abad Area of Qom Province. Amirkabir J civil Eng 52:3237–3248
45. Zomorodian SMA, Ghaffari H, O'Kelly BC (2019) Stabilisation of crustal sand layer using biocementation technique for wind erosion control. Aeolian Res. 40. https://doi.org/10.1016/j.aeolia.2019.06.001
46. Huang J, Kogbara RB, Hariharan N et al (2021) A state-of-the-art review of polymers used in soil stabilization. Constr Build Mater 305
47. Tomar RS, Gupta I, Singhal R, Nagpal AK (2007) Synthesis of poly (Acrylamide-co-acrylic acid) based superaborbent hydrogels: study of network parameters and swelling behaviour. Polym Plast Technol Eng 46. https://doi.org/10.1080/03602550701297095
48. Liu J, Chen Z, Kanungo DP et al (2019) Topsoil reinforcement of sandy slope for preventing erosion using water-based polyurethane soil stabilizer. Eng Geol 252. https://doi.org/10.1016/j.enggeo.2019.03.003
49. Horn R, Taubner H, Wuttke M, Baumgartl T (1994) Soil physical properties related to soil structure. Soil Tillage Res 30. https://doi.org/10.1016/0167-1987(94)90005-1
50. Bai Y, Liu J, Song Z et al (2019) Unconfined compressive properties of composite sand stabilized with organic polymers and natural fibers. Polym (Basel) 11. https://doi.org/10.3390/polym11101576
51. Liu J, Shi B, Jiang H et al (2011) Research on the stabilization treatment of clay slope topsoil by organic polymer soil stabilizer. Eng Geol 117. https://doi.org/10.1016/j.enggeo.2010.10.011
52. Cao Y, Zavattieri P, Youngblood J et al (2016) The relationship between cellulose nanocrystal dispersion and strength. Constr Build Mater 119. https://doi.org/10.1016/j.conbuildmat.2016.03.077
53. Guo A, Sun Z, Sathitsuksanoh N, Feng H (2020) Review a review on the application of nanocellulose in cementitious materials. Nanomaterials 10
54. Sun X, Wu Q, Lee S et al (2016) Cellulose nanofibers as a modifier for Rheology, Curing and Mechanical Performance of Oil Well Cement. Sci Rep 6. https://doi.org/10.1038/srep31654
55. Thuwall M, Boldizar A, Rigdahl M (2006) Extrusion processing of high amylose potato starch materials. Carbohydr Polym 65. https://doi.org/10.1016/j.carbpol.2006.01.033
56. Saieh SE, Eslam HK, Ghasemi E et al (2019) Physical and morphological effects of cellulose nano- fibers and nano-clay on biodegradable WPC made of recycled starch and industrial sawdust. BioResources 14. https://doi.org/10.15376/biores.14.3.5278-5287

57. Almajed A, Tirkolaei HK, Kavazanjian E, Hamdan N (2019) Enzyme Induced Biocementated Sand with High Strength at Low Carbonate Content. Sci Rep 9. https://doi.org/10.1038/s41598-018-38361-1
58. Zare S, Mohammadi J, Mombani M et al (2020) Effect of different mulches on some physical and mechanical properties of aeolian soil. Degrad Rehabilitation Nat Land 1:105–119
59. Diouf B, Skidmore EL, Layton JB, Hagen LJ (1990) Stabilizing fine sand by adding clay: Laboratory wind tunnel study. Soil Technology 3. https://doi.org/10.1016/S0933-3630(05)80014-5
60. Barajas-Ledesma RM, Stocker CW, Wong VNL et al (2022) Biodegradation of a Nanocellulose Superabsorbent and its effect on the growth of spinach (Spinacea oleracea). ACS Agricultural Science and Technology. 2. https://doi.org/10.1021/acsagscitech.1c00178